CONF-881022--1

DE89 002209

DEVELOPMENT OF AN OPTICAL DIGITAL IONIZATION CHAMBER[1]

J. E. Turner, S. R. Hunter, R. N. Hamm, H. A. Wright, Oak Ridge National Laboratory, Post Office Box 2008, Oak Ridge, TN 37831-6123 USA; G. S. Hurst and W. A. Gibson, Pellissippi International, 10521 Research Drive, Knoxville, TN 37932 USA.

We are developing a new device for optically detecting and imaging the track of a charged particle in a gas. The electrons in the particle track are made to oscillate rapidly by the application of an external, short-duration, high-voltage, RF electric field. The excited electrons produce additional ionization and electronic excitation of the gas molecules in their immediate vicinity, leading to copious light emission (fluorescence) from the selected gas, allowing the location of the electrons along the track to be determined. Two digital cameras simultaneously scan the emitted light across two perpendicular planes outside the chamber containing the gas. The information thus obtained for a given track can be used to infer relevant quantities for microdosimetry and dosimetry, e.g., energy deposited, LET, and track structure in the gas. The design of such a device now being constructed and methods of obtaining the dosimetric data from the digital output will be described.

---

[1]Research sponsored by the Office of Health and Environmental Research and the Office of Nuclear Safety, U.S. Department of Energy, under contract DE-AC05-84OR21400 with Martin Marietta Energy Systems, Inc. and by NCI under contract with Pellissippi International.

Introduction

The title of this workshop brings together two aspects of radiation research: the science of microdosimetry and the practice of personnel radiation protection through the use of dose equivalent. The two are historically related through the measurement of LET distributions by microdosimetric methods as pioneered by Rossi[1]. Today, microdosimetry is playing a fundamental role in the consideration of the most suitable reference variable for quality factors and the general expression of radiation quality for radiological protection. Microdosimetry also encompasses the study of fluctuations in energy deposition on a scale of cellular and subcellular - even molecular - dimensions. It is basic to our understanding of instrument response and of cavity and interface problems.

Calculations of charged-particle track structure have become an important part of microdosimetry. It is through such calculations that many measurements are analyzed, evaluated, and compared. Radiations of different quality, for instance, can be characterized in terms of their calculated proximity functions, giving the distribution of distances between ionizations in the track of a particle in a gas or in tissue. By way of example, Fig. 1(a) shows a track segment of a 5-MeV alpha particle in liquid water, calculated with the Monte Carlo computer code OREC[2]. Each dot shows the position of a subexcitation electron, one with an energy less than the assumed threshold of 7.4 eV for electronic transitions in liquid water. This spatial pattern of secondary electrons is formed rapidly (in $\sim 10^{-15}$ s) in the wake of the traversing alpha particle. For contrast, Fig. 1(b) shows the tracks of 1-keV electrons. The figure represents two examples of energy deposition

patterns by radiation. Microdosimetry addresses the ultimate differences in the physical, chemical, and biological effects of radiation in terms of track structure.

While such calculations are a cornerstone of microdosimetry, they are subject to uncertainties that have not been evaluated experimentally. For example, measurements of inelastic and elastic scattering cross sections for low-energy electrons in gases and, especially, in water or tissue are almost wholly lacking. Nevertheless, calculations based on various models can be very useful.

This paper describes the development of a new type of radiation detector which could, in principle, determine the three-dimensional spatial distribution of electrons in the track of a charged particle in a gas. The device is based on the detection of secondary electrons by optical means. Specifically, we hope to measure the numbers of electrons in various volume elements of a gas immediately after traversal by a charged particle. The electron numbers would provide a digital description of the track. Such an instrument would provide measurements for direct comparison with track-structure calculations. Moreover, as discussed below, the principle would have potential uses for measurements of a variety of important quantities for physics and dosimetry. At the present time we have constructed a device in which we have visually observed and photographed alpha-particle tracks. The device and its operation and our plans for continuing development of a digital chamber are described.

Optical Detection of Charged-Particle Tracks

The simple, preliminary device that we have used to optically observe ionizing tracks is shown schematically in Fig. 2. A ^{241}Am source (~1 μCi,

from a smoke detector) emits a 5.5-MeV alpha particle into the chamber gas, leaving a trail of subexcitation electrons in its path. An external, high-frequency (~10 MHz), high-voltage (~20 kV) pulse is applied at intervals of ~0.01 s across two disc-shaped electrodes on either side of the track. The application of the RF field is not triggered by the passage of the alpha particle in the present chamber, but will be in a later device. However, if the RF field happens to be applied immediately after the passage of the alpha particle, then the field rapidly accelerates the electrons back and forth in the particle track, causing them to ionize and excite gas molecules in their immediate vicinity. The excited gas molecules emit light in the UV to visible range by fast fluorescent decay in sufficient quantities for detection. Under suitable conditions, the amount of light from different portions of the track is proportional to the number of subexcitation electrons there, thus providing the basis for a digital characterization of the track. Tracks are readily visible to the naked, dark-adapted eye.

Figure 3 shows a photograph of an alpha-particle track from the ^{241}Am source. The particle starts from the upper right in each panel and stops in the lower left-hand region, where the track is the most dense. The track is about 5 cm long and 3-4 mm in width. The "raw" photograph is shown in the upper left-hand panel. As described in the next section, the panel in the upper right shows the track after it is digitally enhanced. The bottom two panels in the figure, which are identical, are obtained from the picture in the upper right with further enhancement.

Operation of First Chamber

The chamber in Fig. 2 is cylindrical in shape with a height of 3 cm and a diameter of 10 cm. A bottom plate of aluminum is used as one electrode and an

upper plate of tin-oxide coated glass is used as the other. The walls are made of transparent Lucite, permitting viewing of the tracks from the sides as well as from above. The ratio of the field strength and pressure (E/P) is a critical factor in the operation of the system. For a given voltage across the electrodes, this can be changed by changing their separation or the gas pressure in the chamber. Various combinations of gases and pressures were tried. A gas pressure in the neighborhood of 500 torr conveniently gives alpha-particle track lengths of about 7 cm and sufficient vacuum to secure the electrodes firmly to their O-ring seals. The chamber was usually operated at pressures between 300 and 600 torr. It was found necessary to evacuate the chamber to less than 10 mtorr before filling in order to remove contaminating gases, particularly oxygen.

The quantum efficiency and spectral response of light emission from the excited gas depends on the gas and its trace contaminants. Several combinations of gases and pressures have been tried: Ar, N_2, Xe, propane, and TMAE (tetrakis(dimethylamine)ethylene). Argon and nitrogen were used as carrier gases with traces of the other gases added to increase Penning ionization and excitation processes. Nitrogen was also tried as a trace gas in argon. In most cases, the major portion of the light from the excited gas is emitted as UV, which is absorbed in the walls of the chamber and is not visible to the eye. TMAE has a very low ionization potential (5.4 eV vs. 15.7 eV for Ar) and emits visible light of wavelength 480 nm. However, its quantum efficiency is low. It was found that argon with ~1% xenon was the optimum gas mixture in the present experimental apparatus.

The RF field requirement is approximately 20 kV at a frequency of 10 MHz across the chamber electrodes in Fig. 2. The capacitance of the chamber is around 10 pF, and consequently the impedance is $\approx$1500 Ω at 10 MHz. Thus a

peak current in excess of 10 A is needed, but only for a few cycles. For the first device we decided to use a tuned shock-excited transformer, as indicated in the figure. An automotive spark coil and spark module were selected for the high-voltage power supply, triggered at about 100 Hz by a signal generator. The coil output was rated at 30 kV with a rise time of ~100 μs, and it supplied adequate energy for this application. The high-voltage supply charges the capacitor C_1 through the primary L_1 of the transformer. When the breakdown potential is reached, conduction across the spark gap occurs. The primary L_1C_1 circuit then resonates and is damped by dissipative losses. Oscillations are induced in the secondary L_2C_C circuit, where C_C represents the capacitance of the chamber. To maximize energy transfer and to reduce distortions, the primary and secondary circuits are independently tuned to the same resonance frequency. A number of tests were carried out to investigate the effects of the inductance, turn ratios, and different wire diameters and materials on the performance of the device.

Stray inductances and capacitances can cause significant problems. The large RF noise from the spark gap precludes direct observation of the voltage signal across the chamber with an oscilloscope. However, placing the scope probe close to the chamber and observing the induced signal gives a good indication of the shape, frequency, and decay time of the signal impressed on the chamber. If the tuning is accurate, the signal is a damped sine wave. The peak of the second oscillation is typically ~15% lower than the first. Further investigation has indicated that the electronic excitation comes primarily from the first cycle.

As the gas pressure in the chamber is increased from ~30 mtorr to near atmospheric, typical discharge regions are observed without the alpha source present. From no discharge at the lowest pressures, the onset of a glow is

seen as the pressure is increased. Further pressure increase results in well-defined sparks, until the pressure reaches a level at which the chamber no longer continuously conducts. When an alpha-particle track is present, tracks of brilliant streamers, consisting of discharges across the chamber, are observed at pressures where random sparks occurred before. At still higher pressures, where random spark discharges and streamers disappear, alpha-particle tracks are seen as a diffuse blue glow. The gas pressure for optimal track formation is critical and slight changes in E/P are very significant.

Because there is no triggering mechanism to start the RF field in response to the entry of an alpha particle into the chamber, tracks are seen at random times, on the order of seconds apart. Although readily visible to the eye, the tracks are difficult to photograph. In order to increase the film speed, the film was pre-exposed before exposing it to the light from the alpha tracks. Exposures were made by holding the camera shutter open and then closing it after visual observation of a track. Upon developing, most negative frames showed nothing, due to the low levels of light. A few showed discernible tracks. Prints of these, however, did not show a clear image of a track above the pre-fogged background (e.g., upper left frame in Fig. 3). With the assistance of the Electrical Engineering Department of the University of Tennessee and Perceptics, Inc., the track images were digitized and enhanced, enabling results similar to those shown in Fig. 3 to be obtained. The upper-right panel in Fig. 3 was obtained by enhancement with 256 shades of gray. The two bottom panels (identical) were generated from the latter, using only two shades, black and white.

DISCLAIMER

An Optical, Digital Ionization Detector for Microdosimetry

Given the "proof-of-principle" observation and the imaging of alpha-particle tracks by optical detection, we turn next to the development of an instrument for making microdosimetric measurements. Its main features, which are shown schematically in Fig. 4, have been published previously[3]. An ionizing particle leaves a track of secondary electrons between the electrodes, as indicated. The particle also excites gas molecules, which promptly emit a small burst of optical radiation through the decay of excited states. This fluorescence radiation is detected by two wide-angle, fast, high-sensitivity photomultipliers, which feed signals into a fast discriminator coincidence detector. If the two photomultiplier pulses are detected within a given coincidence window time ($\lesssim$ 50 ns), then the detector produces a trigger pulse for the RF field. The trigger pulse is fed into a master timing circuit which, in turn, triggers a high-voltage RF generator, producing the exciting field across the electrodes.

As already mentioned, the intensity of the light emitted depends on the magnitude and duration of the RF burst. The gas should have a high ionizing efficiency (low ionization threshold and low W value) and, more importantly, a high quantum yield for prompt (<10 ns) UV-to-visible radiation. Calculations show that the amplitude and duration of the RF burst can be chosen so that every electron in a track will emit a detectable pulse of light when observed by a camera from any direction.

From observation of the emitted radiation, we envision using two two-dimensional digital cameras, as shown in Fig. 4, which simultaneously view the light output across two perpendicular planes. The cameras could be either silicon-intensified vidicon cameras or microchannel plate-intensified, charge-coupled devices (or similar semiconductor cameras). Large pixel arrays are

required to accurately image the optical radiation from chamber, the resolution being proportional to the size of the pixel arrays in the cameras. The cameras are triggered by a pulse from the master timing circuit. They have adjustable exposure times (10 ns to 1 ms) to ensure that at least one detectable photon is recorded by both cameras for every electron in the track. The two cameras image the track in the two perpendicular planes and digitally store the information. The information is then transferred to a computer for analysis and track reconstruction.

After the imaging of a track is completed, a small DC clearing field is applied to clear the electrons and positive ions out of the chamber. The detection circuits are finally reset to record the next particle. The "cycle time" of the instrument will be on the order of ≈10 ms, so that about 100 events per second could, in principle, be measured. In practice, however, this pace of data acquisition would far outstrip the rate of transfer and analysis. Perhaps one event per second would be a reasonable rate for taking data.

Potential Uses of an Optical Digital Track Detector

The design of a particular chamber to be built would depend upon its intended use. We are now constructing a prototype neutron monitor. The principal track information needed is the energy deposited by an event and the corresponding track length. The energy is proportional to the total light output or the intensity and, under Bragg-Gray conditions, provides a measure of the absorbed dose in the wall of the chamber. The LET (in the gas) is the ratio of the energy deposited and the track length; it is needed to obtain the quality factor and the dose equivalent for the event. Moreover, one does not really need to know the LET when it is large. A quality factor of 20 can be

assigned when LET > 175 keV/μm in water. The unfolding of dosimetric information from recorded optical data appears to be relatively straightforward. In fact, successful algorithms for this purpose, utilizing an analogous digital neutron chamber design, have been worked out in detail[4].

Different demands would be placed on a chamber to be used for microdosimetric measurements. A primary objective of such an instrument would be to measure actual electron positions in a track in a gas, analogous to the calculated positions in water in Fig. 1. The detector would thus give the spatial distribution of events and patterns of energy distribution by the charged particle and all of its secondaries. Calculations indicate that, with present know-how and with presently available (but expensive) digital cameras, it should be possible to image electrons in a track with a position uncertainty of ~1 mm in a gas at a pressure of about 5 torr. This resolution translates to 10×10^{-7} g/cm^2, or ~10 nm in unit density material. (The diameter of the DNA double helix is ~2 nm.) Thus the potential exists for measuring energy deposition in such small volumes, opening up the field of nanodosimetry.

In addition to neutron dosimetry and microdosimetry, an optical detector would have other immediate applications. A number of important quantities for radiation physics could be determined on a track-by-track basis: W values, Fano factors, and energy-loss straggling distributions. Such a detector could also be used for three-dimensional characterization of laser and X-ray beams.

In another potential application, as mentioned in the Introduction, there is considerable discussion of using microdosimetric distributions rather than LET to characterize radiation quality for protection purposes. An improved

operational capability to measure such distributions could have an influence on the formulation of such standards as well as their technological implementation.

References

1. Microdosimetry, ICRU Report 36, International Commission on Radiation Units and Measurements, Bethesda, Maryland (1983).

2. Hamm, R. N., Turner, J. E., Ritchie, R. H., and Wright, H. A., Calculation of Heavy-Ion Tracks in Liquid Water, *Radiat. Res.* 104 (1985) S20 - S-26.

3. Hunter, S. R., Evaluation of a Digital Optical Ionizing Radiation Particle Track Detector, *Nucl. Instr. Meth.* A260 (1987) 469-477.

4. Bolch, Wesley, E., Turner, J. E., Hamm, R. N., Wright, H. A., and Hurst, G. S., A Method of Obtaining Neutron Dose and Dose Equivalent from Digital Measurements and Analysis of Recoil-Particle Tracks, *Health Phys.* 53 (1987) 241-253.

Figure Captions

1. (a) Calculated track segment of a 5-MeV alpha particle in liquid water showing (dots) the locations of all subexcitation electrons (energies <7.4 eV) at 10^{-15} s after passage of the particle.

   (b) 1-keV electron tracks in liquid water at 10^{-15} s.

2. Schematic diagram of the proof-of-principle device for observing alpha particles by optical means.

3. Upper left: Photograph of alpha-particle track. Upper right: Digitally enhanced photo of same by using scale with 256 shades of gray. Bottom panels (same): Further digital enhancement of upper-right panel with only black/white scale.

4. Schematic diagram showing principal components of an instrument that could be used for measurements in microdosimetry and other fields. From Ref. (3).

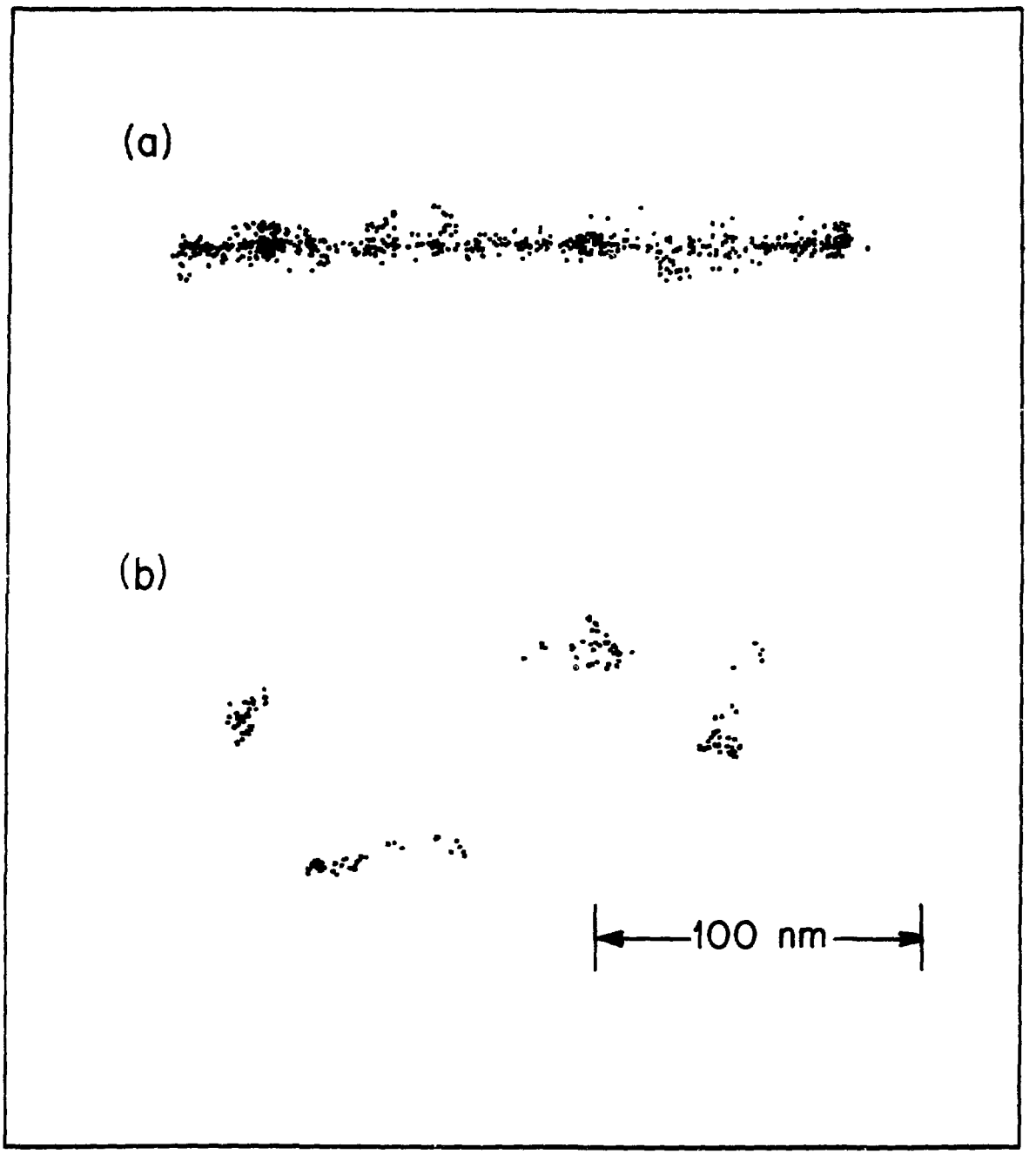
(a)
(b)
100 nm

ORNL-DWG 88M-9029

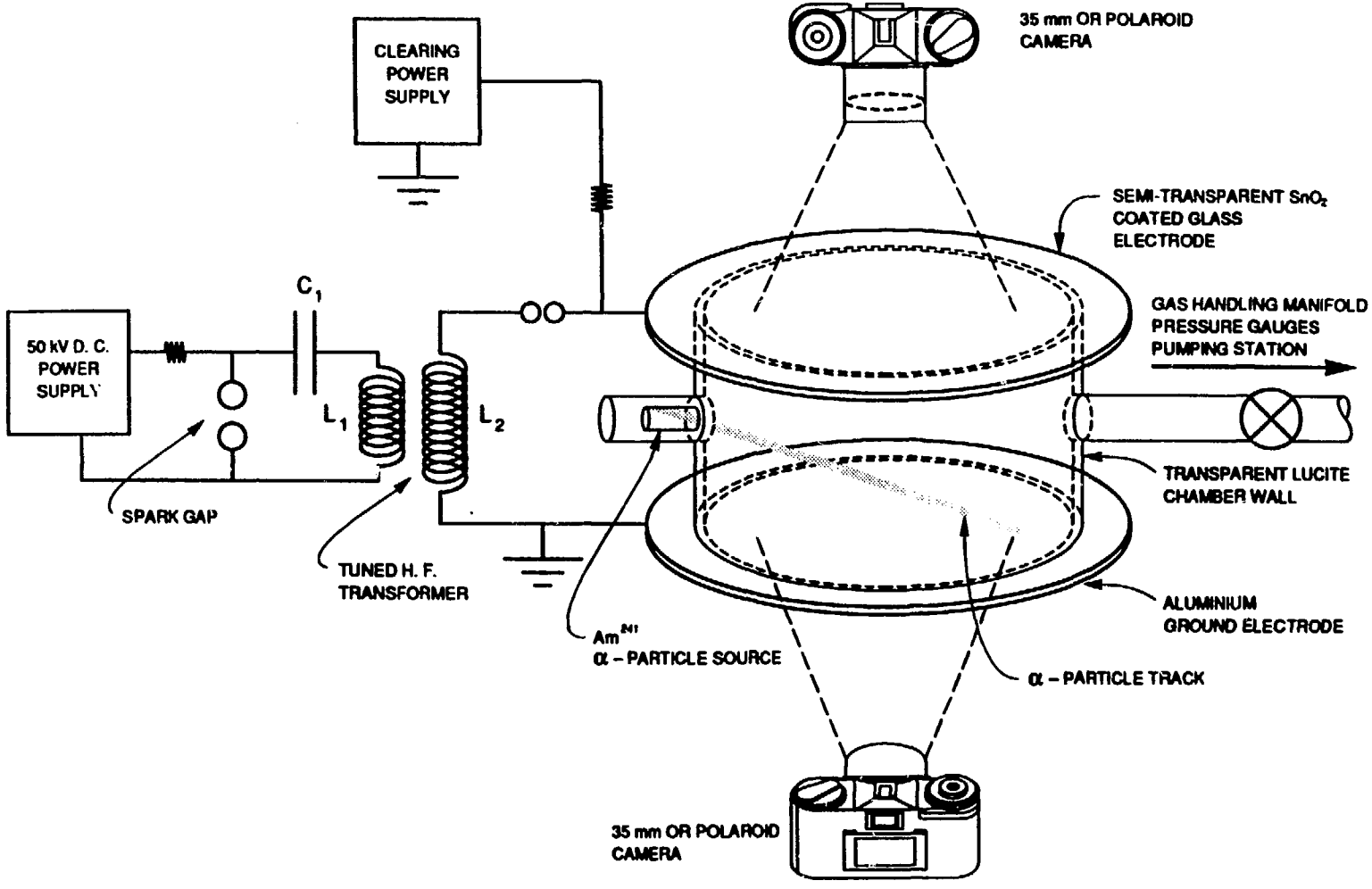

ORNL DWG 86 13108